6

Adaptation and firing patterns

When an experimenter injects a strong step current into the soma of a neuron, the response consists of a series of spikes separated by long or short intervals. The stereotypical arrangement of short, long or very long interspike intervals defines the neuronal *firing pattern*. In Chapter 2 we have already encountered firing patterns such as tonic, adapting, or delayed spike firing. In addition to these, several variants of burst firing have also been observed in real neurons (see Fig. 6.1). This diversity of firing patterns can be explained, to a large extent, by adaptation mechanisms which in turn depend on the zoo of available ion channels (Chapter 2) and neuronal anatomy (Chapter 3).

In order to describe firing patterns, and in particular adaptation, in a transparent mathematical framework, we start in this chapter with the simplified model of spike initiation from Chapter 5 and include a phenomenological equation for subthreshold and spike-triggered adaptation. The resulting model is called the adaptive exponential integrate-and-fire (AdEx; Section 6.1). We then use this simple model to explain the main firing patterns (Section 6.2). In Section 6.3, we describe how the parameters of the subthreshold and spike-triggered adaptation reflect the contribution of various ion channels and of dendritic morphology. Finally, we introduce the Spike Response Model (SRM; Section 6.4) as a transparent framework to describe neuronal dynamics. The Spike Response Model will serve as a starting point for the Generalized Linear Models which we will discuss later, in Chapter 9.

6.1 Adaptive exponential integrate-and-fire

In the previous chapter we have explored nonlinear integrate-and-fire neurons where the dynamics of the membrane voltage is characterized by a function $f(u)$. A single equation is, however, not sufficient to describe the variety of firing patterns that neurons exhibit in response to a step current. We therefore couple the voltage equation to abstract current

https://doi.org/10.1017/CBO9781107447615.008 Published online by Cambridge University Press

variables w_k, each described by a linear differential equation. The set of equations is

$$\tau_m \frac{\mathrm{d}u}{\mathrm{d}t} = f(u) - R\sum_k w_k + RI(t), \tag{6.1}$$

$$\tau_k \frac{\mathrm{d}w_k}{\mathrm{d}t} = a_k\,(u - u_{\rm rest}) - w_k + b_k \tau_k \sum_{t^f} \delta(t - t^f). \tag{6.2}$$

The coupling of voltage to the adaptation current w_k is implemented by the parameter a_k and evolves with time constant τ_k. The adaptation current is fed back to the voltage equation with resistance R. Just as in other integrate-and-fire models, the voltage variable u is reset if the membrane potential reaches the numerical threshold $\Theta_{\rm reset}$. The moment $u(t) = \Theta_{\rm reset}$ defines the firing time $t^f = t$. After firing, integration of the voltage restarts at $u = u_r$. The δ-function in the w_k equations indicates that, during firing, the adaptation currents w_k are increased by an amount b_k. For example, a value $b_k = 10\,\mathrm{pA}$ means that the adaptation current w_k is 10 pA stronger after a spike than it was just before the spike. The parameters b_k are the "jump" of the spike-triggered adaptation. One possible biophysical interpretation of the increase is that during the action potential calcium enters the cell so that the amplitude of a calcium-dependent potassium current is increased. The biophysical origins of adaptation currents will be discussed in Section 6.3. Here we are interested in the dynamics and neuronal firing patterns generated by such adaptation currents. Various choices are possible for the nonlinearity $f(u)$ in the voltage equation. We have seen in the previous chapter (Section 5.2) that the experimental data suggests a nonlinearity consisting of a linear leak combined with an exponential activation term, $f(u) = -(u - u_{\rm rest}) + \Delta_T \exp\left(\frac{u-\vartheta_{\rm rh}}{\Delta_T}\right)$. The adaptive exponential integrate-and-fire model (AdEx) consists of such an exponential nonlinearity in the voltage equation coupled to a single adaptation variable w

$$\tau_m \frac{\mathrm{d}u}{\mathrm{d}t} = -(u - u_{\rm rest}) + \Delta_T \exp\left(\frac{u - \vartheta_{\rm rh}}{\Delta_T}\right) - R\,w + RI(t), \tag{6.3}$$

$$\tau_w \frac{\mathrm{d}w}{\mathrm{d}t} = a\,(u - u_{\rm rest}) - w + b\tau_w \sum_{t^f} \delta(t - t^f)\,. \tag{6.4}$$

At each threshold crossing the voltage is reset to $u = u_r$ and the adaptation variable w is increased by an amount b. Adaptation is characterized by two parameters: the parameter a is the source of subthreshold adaptation because it couples adaptation to the voltage. Spike-triggered adaptation is controlled by a combination of a and b. The choice of a and b largely determines the firing patterns of the neuron (Section 6.2) and can be related to the dynamics of ion channels (Section 6.3). Before exploring the AdEx model further, we discuss two other examples of adaptive integrate-and-fire models.

Example: Izhikevich model

While the AdEx model exhibits the nonlinearity of the exponential integrate-and-fire model, the Izhikevich model uses the quadratic integrate-and-fire model for the first

https://doi.org/10.1017/CBO9781107447615.008 Published online by Cambridge University Press

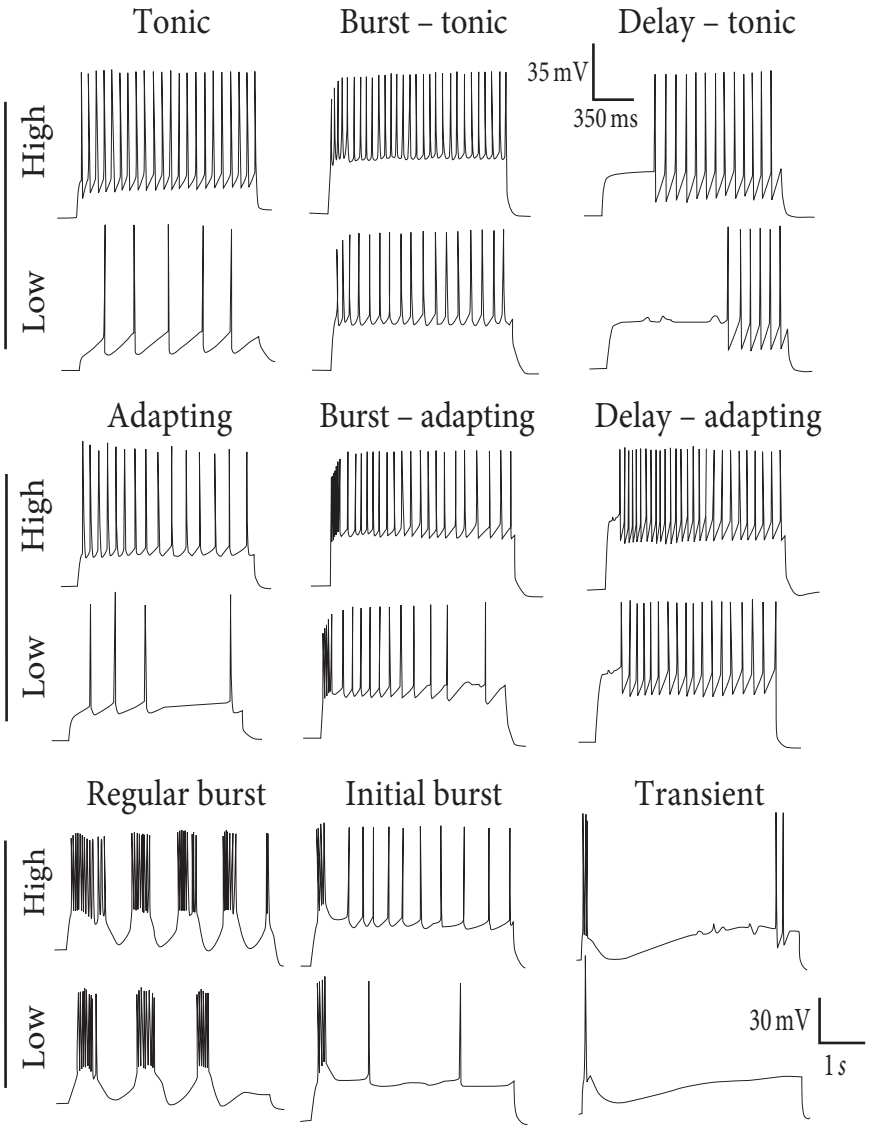

Fig. 6.1 Multiple firing patterns in cortical neurons. For each type, the neuron is stimulated with a step current with low or high amplitude. Modified from Markram *et al*. (2004).

equation

$$\tau_m \frac{\mathrm{d}u}{\mathrm{d}t} = (u - u_{\mathrm{rest}})(u - \vartheta) - Rw + RI(t), \tag{6.5}$$

$$\tau_w \frac{\mathrm{d}w}{\mathrm{d}t} = a(u - u_{\mathrm{rest}}) - w + b\tau_w \sum_{t^f} \delta(t - t^f). \tag{6.6}$$

https://doi.org/10.1017/CBO9781107447615.008 Published online by Cambridge University Press

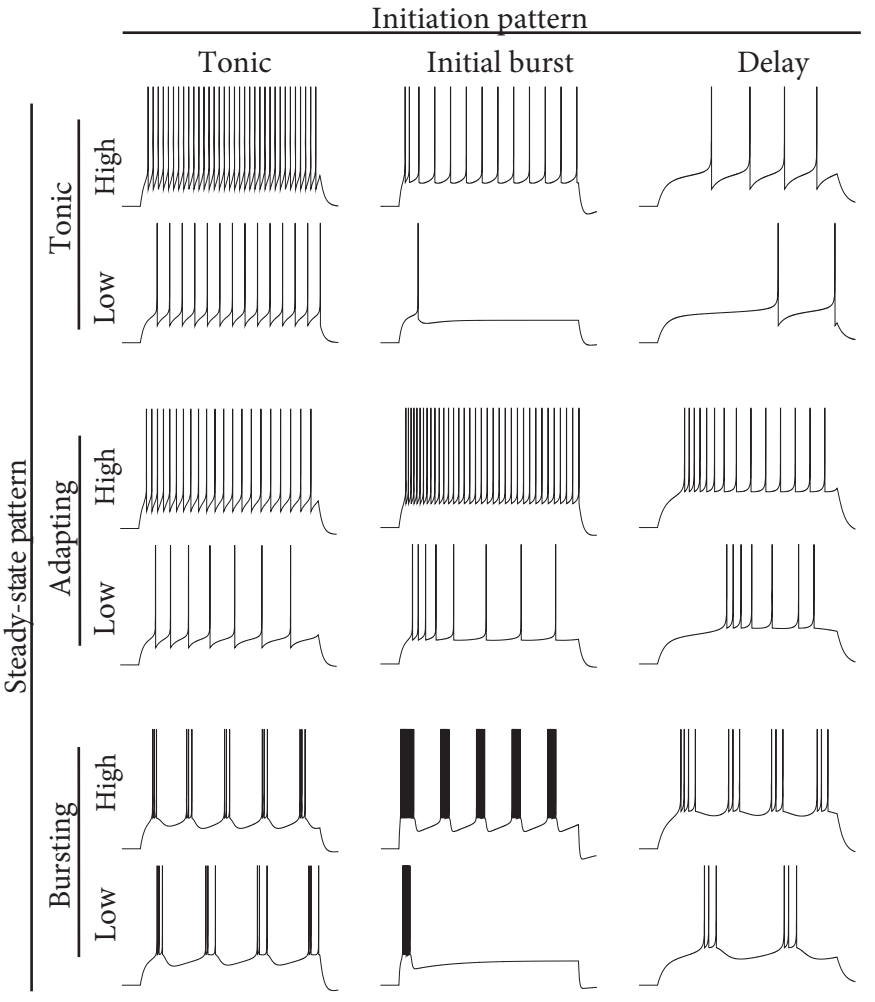

Fig. 6.2 Multiple firing patterns in the AdEx neuron model. For each set of parameters, the model is stimulated with a step current with low or high amplitude. The spiking response can be classified by the steady-state firing behavior (vertical axis: tonic, adapting, bursting) and by its transient initiation pattern as shown along the horizontal axis: tonic (i.e., no special transient behavior), initial burst, or delayed spike initiation.

If $u = \theta_{\text{reset}}$, the voltage is reset to $u = u_r$ and the adaptation variable w is increased by an amount b. Normally b is positive, but $b < 0$ is also possible.

Example: Leaky model with adaptation

Adaptation variables w_k can also be combined with a standard leaky integrate-and-fire

https://doi.org/10.1017/CBO9781107447615.008 Published online by Cambridge University Press

Type	Fig.	τ_m (ms)	a (nS)	τ_w (ms)	b (pA)	u_r (mV)
Tonic	6.3a	20	0.0	30.0	60	−55
Adapting	6.3b	200	0.0	100	5.0	−55
Init. burst	6.4a	5.0	0.5	100	7.0	−51
Bursting	6.4c	5.0	−0.5	100	7.0	−46
Irregular	6.5a	9.9	−0.5	100	7.0	−46
Transient	6.9a	10	1.0	100	10	−60
Delayed	6.9c	5.0	−1.0	100	10	−60

Table 6.1 *Exemplar parameters for the AdEx model. In all cases, the resting potential was* $u_{\rm rest} = -70\,{\rm mV}$*, the resistance was* $R = 500\,{\rm M\Omega}$*, the threshold was* $\vartheta_{\rm rh} = -50\,{\rm mV}$ *with sharpness* $\Delta_T = 2\,{\rm mV}$*, and the current step was fixed to* 65 pA *except for "delayed" where it was at* 25 pA.

model

$$\tau_m \frac{{\rm d}u}{{\rm d}t} = -(u - u_{\rm rest}) - R\sum_k w_k + RI(t), \tag{6.7}$$

$$\tau_k \frac{{\rm d}w_k}{{\rm d}t} = a\,(u - u_{\rm rest}) - w_k + b_k \tau_k \sum_{t^f} \delta(t - t^f). \tag{6.8}$$

At the moment of firing, defined by the threshold condition $u(t^f) = \theta_{\rm reset}$, the voltage is reset to $u = u_r$ and the adaptation variables w_k are increased by an amount b_k. Note that in the leaky integrate-and-fire model the numerical threshold $\theta_{\rm reset}$ coincides with the voltage threshold ϑ that one would find with short input current pulses.

6.2 Firing patterns

The AdEx model is capable of reproducing a large variety of firing patterns that have been observed experimentally. In this section, we show some typical firing patterns, and show how the patterns can be understood mathematically, adapting the tools of phase plane analysis previously encountered in Chapter 4.

6.2.1 Classification of firing patterns

How are the firing patterns classified? Across the vast field of neuroscience and over more than a century of experimental work, different classification schemes have been proposed. For a rough qualitative classification (Fig. 6.2, exemplar parameters in Table 6.1), it is advisable to separate the steady-state pattern from the initial transient phase (Markram *et al.*, 2004). The initiation phase refers to the firing pattern right after the onset of the

https://doi.org/10.1017/CBO9781107447615.008 Published online by Cambridge University Press

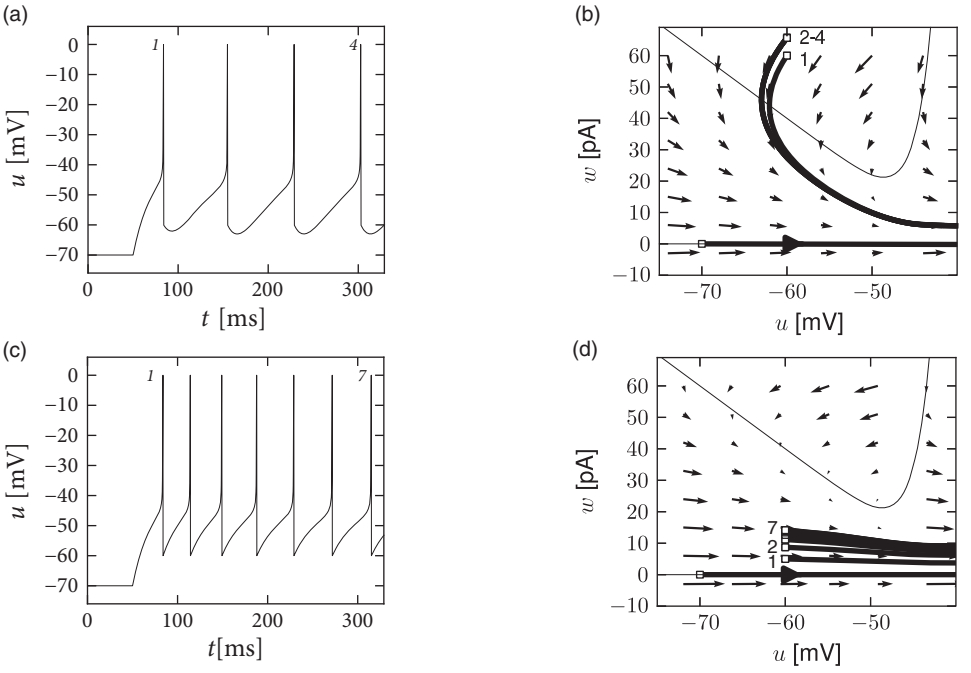

Fig. 6.3 Tonic and adapting firing patterns in the AdEx model. (a) Tonic spiking with a strong spike-triggered current ($b = 60$ pA) of short duration ($\tau_w = 30$ ms). (b) If the reset (empty squares) leads to a value above the u-nullcline, the trajectories make a detour to lower values of u. (c) Spike-frequency adaptation with a weak spike-triggered current ($b = 5$ pA) and slow decay ($\tau_w = 100$ ms). (d) If the reset lands below the u-nullcline, the membrane potential immediately increase towards the next spike. Parameters in Table 6.1.

current step. There are three main initiation patterns: the initiation cannot be distinguished from the rest of the spiking response (tonic); the neuron responds with a significantly greater spike frequency in the transient (initial burst) than in the steady state; the neuronal firing starts with a delay (delay).

After the initial transient, the neuron exhibits a steady-state pattern. Again there are three main types: regularly spaced spikes (tonic); gradually increasing interspike intervals (adapting); or regular alternations between short and long interspike intervals (bursting). Irregular firing patterns are also possible in the AdEx model, but their relation to irregular firing patterns in real neurons is less clear because of potential noise sources in biological cells (Chapter 7). The discussion in the next sections is restricted to deterministic models.

Example: Tonic, adapting and facilitating

When the subthreshold coupling a is small and the voltage reset is low ($u_r \approx u_{\text{rest}}$),

https://doi.org/10.1017/CBO9781107447615.008 Published online by Cambridge University Press

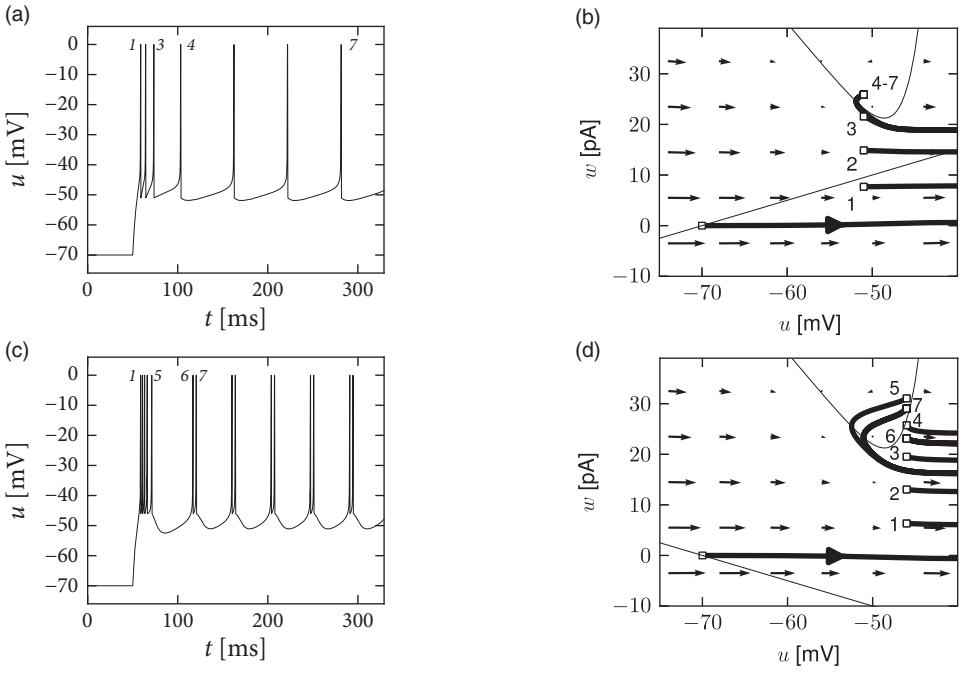

Fig. 6.4 Phase plane analysis of initial bursting and sustained bursting patterns. (a) Voltage trace of an AdEx model with parameters producing an initial burst. (b) In the phase plane, the initial burst is generated by a series of resets below the u-nullcline. Only the fourth reset arrives above the u-nullcline. (c) Voltage trace of an AdEx model exhibiting regular bursts. (d) The phase plane for regular bursting is similar to those of initial burst, except that the first reset above the u-nullcline yields a trajectory that travels below at least one of the previous resets. Hence, the neuron model alternates between direct and detour resets.

the AdEx response is either tonic or adapting. This depends on the two parameters regulating the spike-triggered current: the jump b and the time scale τ_w. A large jump with a small time scale creates evenly spaced spikes at low frequency (Fig. 6.3a). On the other hand, a small spike-triggered current decaying on a long time scale can accumulate strength over several spikes and therefore successively decreases the net driving current $I - w$ (Fig. 6.3b). In general, weak but long-lasting spike-triggered currents cause spike-frequency adaptation, while short but strong currents lead only to a prolongation of the refractory period. There is a continuum between purely tonic spiking and strongly adapting.

Similarly, when the spike-triggered current is depolarizing ($b < 0$) the interspike interval may gradually decrease, leading to spike-frequency facilitation.

https://doi.org/10.1017/CBO9781107447615.008 Published online by Cambridge University Press

6.2.2 Phase plane analysis of nonlinear integrate-and-fire models in two dimensions

Phase plane analysis, which has been a useful tool to understand the dynamics of the reduced Hodgkin–Huxley model (Chapter 4), is also helpful to illustrate the dynamics of the AdEx model. Let us plot the two state variables $u(t)$ and $w(t)$ in the plane and indicate the regions where $\dot{u} = 0$ (u-nullcline) and $\dot{w} = 0$ (w-nullcline) with solid lines.

In the AdEx model, the nullclines look similar to the one-dimensional figures of the exponential integrate-and-fire model in Chapter 5. The u-nullcline is again linear in the subthreshold regime and rises exponentially when u is close to ϑ. Upon current injection, the u-nullcline is shifted vertically by an amount proportional to the magnitude of the current I. The w-nullcline is a straight line with a slope tuned by the parameter a. If there is no coupling between the adaptation variable and the voltage in the subthreshold regime ($a = 0$), then the w-nullcline is horizontal. The fixed points are the points where the curved u-nullcline intersects with the straight w-nullcline. Solutions of the system of differential equations (6.3) and (6.4) appear as a trajectory in the (u, w)-plane.

In constrast to the two-dimensional models in Chapter 4, the AdEx model exhibits a reset which correspond to a jump of the trajectory. Each time the trajectory reaches $u = \theta_{\text{reset}}$, it will be reinitialized at a reset value $(u_r, w + b)$ indicated by an empty square (Fig. 6.3). We note that for the voltage variable the reinitialization occurs always at the same value $u = u_r$; for the adaptation variable, however, the reset involves a vertical shift upwards by an amount b compared with the value of w just before the reset. Thus, the reset maps w to a potentially new initial value after each firing.

There are three regions of the phase plane with qualitatively different ensuing dynamics. These regions are distinguished by whether the reset point is in a region where trajectories are attracted to the stable fixed point or not; and whether the reset is above or below the u-nullcline. Trajectories attracted to a fixed point will simply converge to it. Trajectories not attracted to a fixed point all go eventually to θ_{reset} but they can do so directly or with a detour. A detour is introduced whenever the reset falls above the u-nullcline, because in the area above the u-nullcline the derivative is $\dot{u} < 0$ so that the voltage $u(t)$ must first decrease before it can eventually increase again. Thus a "detour reset" corresponds to a downswing of the membrane potential after the end of the action potential. The distinction between detour and direct resets is helpful to understand how different firing patterns arise. Bursting, for instance, can be generated by a regular alternation between direct resets and detour resets.

Example: Bursting

Before considering regular bursting, we describe the dynamics of an initial burst. By definition, an initial burst means a neuron first fires a group of spikes at a considerably higher spiking frequency than the steady-state frequency (Fig. 6.4a). In the phase plane, initial bursting is caused by a series of one or more direct resets followed by detour resets (Fig. 6.4b). This firing pattern may appear very similar to strong adaptation where

https://doi.org/10.1017/CBO9781107447615.008 Published online by Cambridge University Press

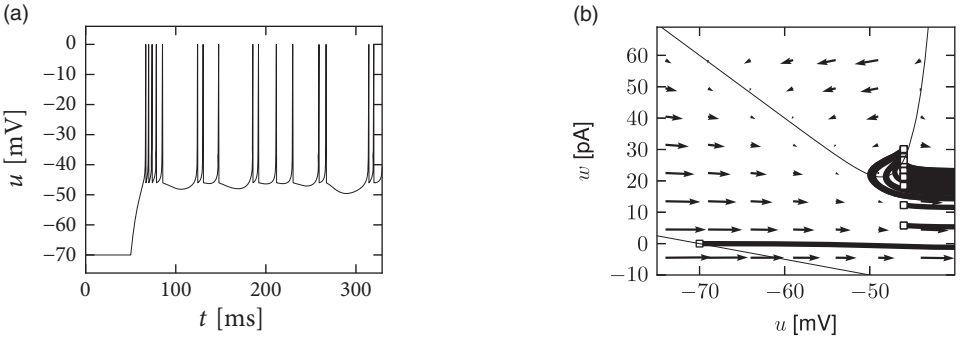

Fig. 6.5 Phase plane analysis of an irregular firing pattern. (a) Voltage trace of an AdEx model showing irregularly spaced spikes. (b) The evolution of trajectories in the phase plane during the simulation in (a) shows that the model switches irregularly between direct and detour resets.

the first spikes also have a larger frequency, but the shape of the voltage trajectory after the end of the action potential (downswing or not) can be used to distinguish between adapting (strictly detour or strictly direct resets) and initial bursting (first direct then detour resets).

Regular bursting can arise from a similar process, by alternation between direct and detour resets. In the phase plane, regular bursting is made possible by a reset u_r higher than the effective threshold ϑ. After a series of direct resets, the first reset that falls above the u-nullcline must make a large detour and is forced to pass under the u-nullcline. When this detour trajectory is mapped below at least one of the previous reset points, the neuron may burst again (Fig. 6.4b).

While the AdEx can generate a regular alternation between direct and detour resets, it can also produce an irregular alternation (Fig. 6.5). Such irregular firing patterns can occur in the AdEx model despite the fact that the equations are deterministic. The aperiodic mapping between the two types of reset is a manifestation of chaos in the discrete map (Naud *et al.*, 2008; Touboul and Brette, 2008). This firing pattern appears for a restricted set of parameters such that, unlike regular and initial bursting, it occupies a small and patchy volume in parameter space.

6.2.3 Exploring the space of reset parameters

The AdEx model in the form of Eqs. (6.3) and (6.4) has nine parameters. Some combinations of parameters lead to initial bursting, others to adaptation, yet others to delayed spike onset, and so on. As we change parameters, we find that each firing pattern occurs in a restricted region of the nine-dimensional parameter space – and this can be labeled by the corresponding firing pattern, e.g., bursting, initial bursting, or adaptive. While inside a given region the dynamics of the model can exhibit small quantitative changes; the big qualitative changes occur at the transition from one region of parameter space to the next.

https://doi.org/10.1017/CBO9781107447615.008 Published online by Cambridge University Press

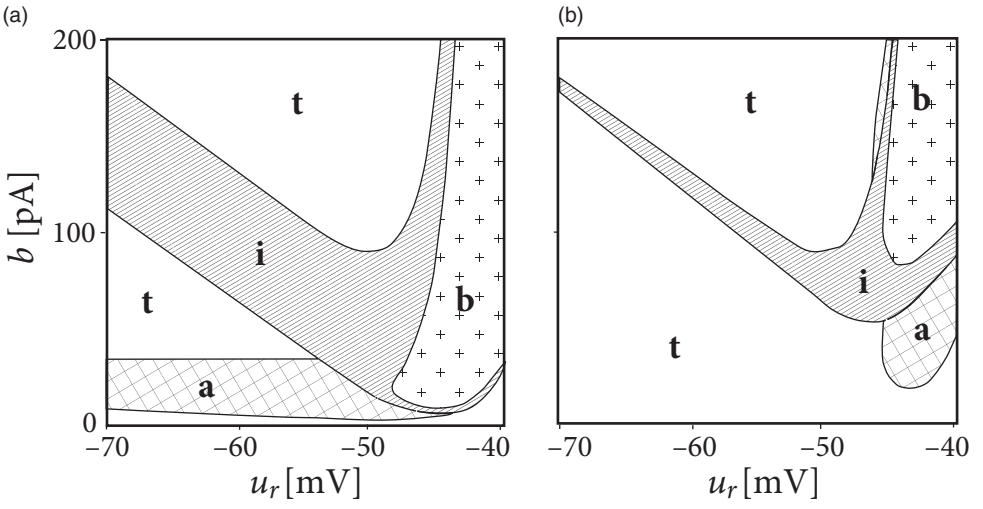

Fig. 6.6 Parameter space of the AdEx model. (a) Combinations of the voltage reset u_r and of the spike-triggered jump b of the adaptation current leading to a tonic (**t**), adapting (**a**), initial burst (**i**) and bursting (**b**) firing patterns for a long adaptation time constant ($\tau_w = 100$ ms) and small subthreshold coupling ($a = 0.001$ nS). (b) Same as (a) but for $\tau_w = 5$ ms. Current was switched from zero to twice the rheobase current and all other parameters are fixed at $\tau_m = 10$ ms, $R = 100\,\mathrm{M\Omega}$, $u_{\rm rest} = -70$ mV, $\vartheta_{\rm rh} = -50$ mV and $\Delta_T = 2$ mV.

Thus, boundaries in the parameter space mark transitions between different types of firing pattern – which are often correlated with types of cells.

To illustrate the above concept of regions inside the parameter space, we apply a step current with an amplitude twice as large as the minimal current necessary to elicit a spike and study the dependence of the observed firing pattern on the reset parameters u_r and b (Fig. 6.6). All the other parameters are kept fixed. We find that the line separating initial bursting and tonic firing resembles the shape of the u-nullcline. This is not unexpected given that the location of the reset with respect to the u-nullcline plays an important role in determining whether the reset is "direct" or leads to a "detour." Regular bursting is possible, if the voltage reset u_r is located above the voltage threshold ϑ. Irregular firing patterns are found within the bursting region of the parameter space. Adapting firing patterns occur only over a restricted range of jump amplitudes b of the spike-triggered adaptation current.

Example: Piecewise-linear model (*)

In order to understand the location of the boundaries in parameter space we consider a piecewise-linear version of the AdEx model

$$f(u) = \begin{cases} -(u - u_{\rm rest}) & \text{if } u \le \vartheta_{\rm rh}, \\ \Delta_T (u - u_p) & \text{otherwise}, \end{cases} \tag{6.9}$$

https://doi.org/10.1017/CBO9781107447615.008 Published online by Cambridge University Press

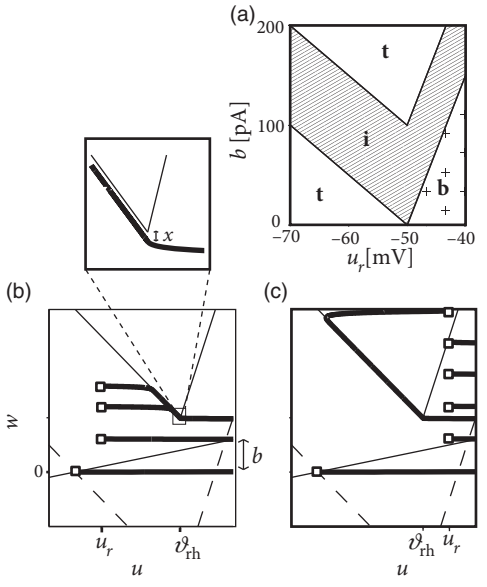

Fig. 6.7 Piecewise-linear model. (a) Parameter space analogous to Fig. 6.6 but for the piecewise-linear model. (b) Evolution of the trajectory (thick solid lines) in the phase plane during tonic spiking. Open squares indicate the initial condition and resets after the first, second, and third spike. Nullclines drawn as thin solid lines. The trajectories follow the u-nullcline at a distance x (inset). The u-nullcline before the application of the step current is shown with a dashed line. (c) As in (b), but during regular bursting.

with

$$u_p = \vartheta_{\rm rh} + \frac{\vartheta_{\rm rh} - u_{\rm rest}}{\Delta_T}, \tag{6.10}$$

which we insert into the voltage equation $\tau_m {\rm d}u/{\rm d}t = f(u) + RI - Rw$; compare Eq. (6.1) with a single adaptation variable of the form (6.2). Note that the u-nullcline is given by $w = f(u)/R + I$ and takes at $u = \vartheta_{\rm rh}$ its minimum value $w_{\rm min} = f(\vartheta_{\rm rh})/R + I$.

We assume separation of time scale ($\tau_m/\tau_w << 1$) and exploit the fact that the trajectories in the phase plane are nearly horizontal (w takes a constant value) – unless they approach the u-nullcline. In particular, all trajectories that start at a value $w_r < w_{\rm min}$ stay horizontal and pass unperturbed below the u-nullcline.

To determine the firing pattern, we need to map the initial condition (u_r,w_r) after a first reset to the value w_e of the adaptation variable at the end of the trajectory: $w_e = M(u_r, w_r)$. The next reset starts then from (u_r,$w_e + b$) and with the help of the mapping function M we can iterate the above procedure. We know already that all trajectories with $w_r < w_{\rm min}$ remain horizontal, so that $w_e = w_r$.

The more interesting situation is $w_r > w_{\rm min}$. We distinguish two possible cases. The first one corresponds to a voltage reset below the threshold, $u_r < \vartheta_{\rm rh}$. A trajectory initiated at $u_r < \vartheta_{\rm rh}$ evolves horizontally until it comes close to the left branch of the u-nullcline. It then follows the u-nullcline at a small distance $x(u)$ below it (see Section 4.6). This distance can be shown to be

$$x(u) = \frac{\tau_m}{\tau_w} \left[I - (a + R^{-1})(u - u_{\rm rest}) \right] , \tag{6.11}$$

https://doi.org/10.1017/CBO9781107447615.008 Published online by Cambridge University Press

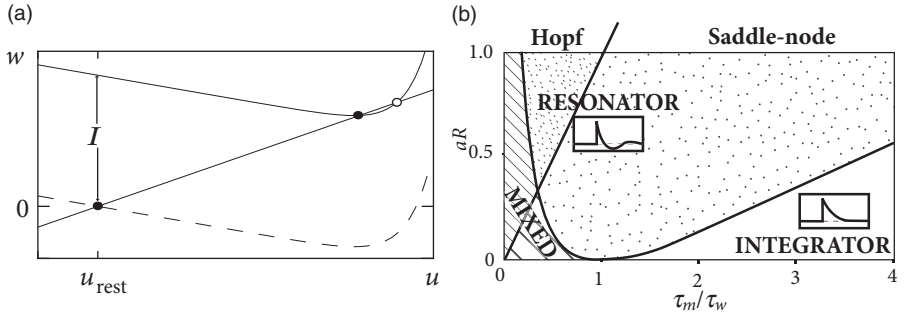

Fig. 6.8 Hopf bifurcation and space of subthreshold parameters. (a) Nullclines and fixed points (filled and open circles) during a Hopf bifurcation. A step current I shifts the u-nullcline upward (solid line). The stability of the stable fixed point (filled circle) is lost in a Hopf bifurcation before the two fixed points merge. If it is not lost before the merge then the bifurcation is saddle-node. (b) The ratio of time constants τ_m/τ_w (horizontal axis) and the factor aR which controls the coupling between voltage and adaptation. The straight diagonal line separates the region where the stationary state of the system loses stability through a Hopf bifurcation ($aR > \tau_m/\tau_w$) from the region of saddle-node bifurcation. The linear response of the subthreshold dynamics is characterized as resonator (dotted region), integrator (blank), or mixed (stripes).

which vanishes in the limit $\tau_m/\tau_w \to 0$. When the u-nullcline reaches its minimum, the trajectory is again free to evolve horizontally. Therefore the final w-value of the trajectory is the one it takes at the minimum of the u-nullcline, so that for $u_r < \vartheta_{\text{rh}}$

$$M(u_r, w_r) = \begin{cases} w_r & \text{if } w_r < f(\vartheta_{\text{rh}})/R + I, \\ f(\vartheta_{\text{rh}})/R + I & \text{otherwise.} \end{cases} \tag{6.12}$$

If $u_r > \vartheta_{\text{rh}}$ then we have a direct reset (i.e., movement starts to the right) if (u_r, w_r) lands below the right branch of the u-nullcline (Fig. 6.7c) and a detour reset otherwise

$$M(u_r, w_r) = \begin{cases} w_r & \text{if } w_r < f(u_r)/R + I, \\ f(\vartheta_{\text{rh}})/R + I & \text{otherwise.} \end{cases} \tag{6.13}$$

The map M uniquely defines the firing pattern. Regular bursting is possible only if $u_r > \vartheta_{\text{rh}}$ and $b < f(u_r) - f(\vartheta_{\text{rh}})$ so that at least one reset in each burst lands below the u-nullcline (Fig. 6.7a). For $u_r > \vartheta_{\text{rh}}$, we have tonic spiking with detour resets when $b > f(u_r) + I$ and initial bursting if $f(u_r) + I > b > f(u_r) - f(\vartheta_{\text{rh}}) + x(\vartheta_{\text{rh}})$.

If $u_r \leq \vartheta$ we have tonic spiking with detour resets when $b > f(u_r) + I$, tonic spiking with direct reset when $b < f(u_r) - f(\vartheta_{\text{rh}})$ and initial bursting if $f(u_r) + I > b > f(u_r) - f(\vartheta_{\text{rh}})$. Note that the rough layout of the parameter regions in Fig. 6.7a, which we just calculated analytically, matches qualitatively the organization of the parameter space in the AdEx model (Fig. 6.6).

https://doi.org/10.1017/CBO9781107447615.008 Published online by Cambridge University Press

6.2.4 Exploring the space of subthreshold parameters

While the exponential integrate-and-fire model loses stability always via a saddle-node bifurcation, the AdEx can become unstable either via a Hopf or a saddle-node bifurcation. Thus, we see again that the addition of an adaptation variable leads to a much richer dynamics.

In the absence of external input, the AdEx has two fixed points, a stable one at $u_{\rm rest}$ and an unstable one at some value $u > \vartheta_{\rm rh}$. We recall from Chapter 4 that a gradual increase of the driving current corresponds to a vertical shift of the u-nullcline (Fig. 6.8a), and to a slow change in the location of the fixed points. The stability of the fixed points, and hence the potential occurrence of a Hopf bifurcation, depends on the slope of the u- and w-nullclines. In the AdEx, an eigenvalue analysis shows that the stable fixed point loses stability via a Hopf bifurcation if $aR > \tau_m/\tau_w$. Otherwise, when the coupling from voltage to adaptation (parameter a) and back from adaptation to voltage (parameter R) are both weak ($aR < \tau_m/\tau_w$), an increase in the current causes the stable fixed point to merge with the unstable one, so that both disappear via a saddle-node bifurcation – just like in the normal exponential integrate-and-fire model. Note, however, that the type of bifurcation has no influence on the firing pattern (bursting, adapting, tonic), which depends mainly on the choice of reset parameters.

However, the subthreshold parameters do control the presence or absence of oscillations in response to a short current pulse. A model showing damped oscillations is often called a *resonator* while a model without is called an *integrator*. We have seen in Chapter 4 that Hopf bifurcations are associated with damped oscillations, but this statement is valid only close to the bifurcation point or rheobase-threshold. The properties can be very different far from the threshold. Indeed, the presence of damped oscillations depends nonlinearly on a/g_L and τ_m/τ_w as summarized in Fig. 6.8b. The frequency of the damped oscillation is given by

$$\omega = \frac{4}{\tau_w}\left[aR - \frac{2\tau_w}{\tau_m}\left(1 - \frac{\tau_m}{\tau_w}\right)^2\right]. \tag{6.14}$$

Example: Transient spiking

Upon the onset of a current step, some neurons may fire a small number of spikes and then remain silent, even if the stimulus is maintained for a very long time. An AdEx model with subthreshold coupling $a > 0$ can explain this phenomenon whereas pure spike-triggered adaptation ($a = 0; b > 0$) cannot account for it, because adaptation would eventually decay back to zero so that the neuron fires another spike.

To understand the role of subthreshold coupling, let us choose parameters a and τ_w such that the neuron is in the resonator regime. The voltage response to a step input then exhibits damped oscillations (Fig. 6.9a). Similar to the transient spiking in the Hodgkin–Huxley model, the AdEx can generate a transient spike if the peak of the

https://doi.org/10.1017/CBO9781107447615.008 Published online by Cambridge University Press

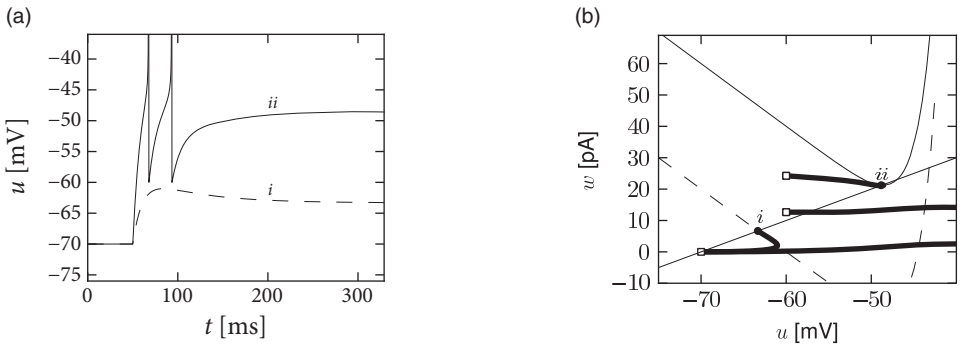

Fig. 6.9 Phase plane analysis of transient spiking in the AdEx model. (a) Voltage trace of an AdEx model with parameters producing transient spiking upon a strong step current input (solid line marked *ii*). A weaker step input generates damped oscillations (dashed line marked *i*). (b) Phase plane with nullclines after application of the strong (solid lines: u- and w-nullclines) or weak step current (dashed line: u-nullcline). Upon injection of the weak step, the stable fixed point is reached after a short transient. Upon injection of the strong current, a stable fixed point remains, but the initial state is outside the region where it would be attracted to the stable fixed point. Only after the second reset (open squares), does the trajectory converge to the fixed point.

oscillation is sufficient to reach the firing threshold. Phase plane analysis reveals that sometimes several resets are needed before the trajectory is attracted towards the fixed point (Fig. 6.9b). In Chapter 2, damped oscillations were due to sodium channel inactivation or I_h. Indeed, the subthreshold coupling can be seen as a simplification of I_h, but many other biophysical mechanisms can be responsible.

6.3 Biophysical origin of adaptation

We have introduced, in Section 6.1, formal adaptation variables w_k which evolve according to a linear differential equation (6.2). We now show that the variables w_k can be linked to the biophysics of ion channels and dendrites.

6.3.1 Subthreshold adaptation by a single slow channel

First we focus on one variable w at a time and study its *subthreshold* coupling to the voltage. In other words, the aim is to give a biophysical interpretation of the parameters a, τ_w, and the variable w that show up in the adaptation equation

$$\tau_w \frac{\mathrm{d}w}{\mathrm{d}t} = a\,(u - E_0) - w\,. \tag{6.15}$$

The biophysical components of *spike-triggered* adaptation (i.e., the interpretation of the reset parameter b) is deferred to Section 6.3.2. Here and in the following we write E_0 instead of $u_{\rm rest}$ in order to simplify notation and keep the treatment slightly more general.

https://doi.org/10.1017/CBO9781107447615.008 Published online by Cambridge University Press

As discussed in Chapter 2, neurons contain numerous ion channels (Section 2.3). Rapid activation of the sodium channels, important during the upswing of action potentials, is well approximated (Fig. 5.4) by the exponential nonlinearity in the voltage equation of the AdEx model, Eq. (6.3). We will see now that the subthreshold current w is linked to the dynamics of other ion channels with a slower dynamics.

Let us focus on the model of a membrane with a leak current and a single, slow, ion channel, say a potassium channel of the Hodgkin–Huxley type

$$\tau_m \frac{\mathrm{d}u}{\mathrm{d}t} = -(u - E_\mathrm{L}) - R_\mathrm{L}\, g_\mathrm{K}\, n^p\, (u - E_\mathrm{K}) + R_\mathrm{L}\, I_\mathrm{ext}, \tag{6.16}$$

where R_L and E_L are the resistance and reversal potential of the leak current, $\tau_m = R_L C$ is the membrane time constant, g_K the maximal conductance of the open channel and n the gating variable (which appears with arbitrary power p) with dynamics

$$\frac{\mathrm{d}n}{\mathrm{d}t} = -\frac{n - n_0(u)}{\tau_n(u)}. \tag{6.17}$$

As long as the membrane potential stays below threshold, we can linearize the equations (6.16) and (6.17) around the resting voltage E_0, given by the fixed point condition

$$E_0 = \frac{E_\mathrm{L} + (R_\mathrm{L}\, g_\mathrm{K})\, n_0(E_0)^p\, E_\mathrm{K}}{1 + (R_\mathrm{L}\, g_\mathrm{K})\, n_0(E_0)^p}. \tag{6.18}$$

The resting potential is shifted with respect to the leak reversal potential if the channel is partially open at rest, $n_0(E_0) > 0$. We introduce a parameter $\beta = g_K\, p\, n_0(E_0)^{p-1}\, (E_0 - E_\mathrm{K})$ and expand $n_0(u) = n_0(E_0) + n_0'\, (u - E_0)$ where n_0' is the derivative dn_0/du evaluated at E_0.

The variable $w = \beta\, [n - n_0(E_0)]$ then follows the linear equation

$$\tau_n(E_0) \frac{\mathrm{d}w}{\mathrm{d}t} = a\,(u - E_0) - w. \tag{6.19}$$

We emphasize that the time constant of the variable w is given by the time constant of the channel at the resting potential. The parameter a is proportional to the sensitivity of the channel to a change in the membrane voltage, as measured by the slope $\mathrm{d}n_0/\mathrm{d}u$ at the equilibrium potential E_0.

The adaptation variable w is coupled into the voltage equation in the standard form

$$\tau_m^\mathrm{eff} \frac{\mathrm{d}u}{\mathrm{d}t} = -(u - E_0) - R\, w + R\, I_\mathrm{ext}. \tag{6.20}$$

Note that the membrane time constant and the resistance are rescaled by a factor $[1 + (R_L\, g_K)\, n_0(E_0)^p\,]^{-1}$ with respect to their values in the passive membrane equation, Eq. (6.16). In fact, both are smaller because of partial opening of the channel at rest.

In summary, each channel with nonzero slope $\mathrm{d}n_0/\mathrm{d}u$ at the equilibrium potential E_0 gives rise to an effective adaptation variable w. Since there are many channels, we can expect many variables w_k. Those with similar time constants can be summed and grouped into a single equation. But if time constants are different by an order of magnitude or more,

https://doi.org/10.1017/CBO9781107447615.008 Published online by Cambridge University Press

Type	Fig.	Act./inact.	τ_w (ms)	β (pA)	a (nS)	δ_x	b (pA)
I_{Na}	2.3	inact.	20	−120	5.0	–	–
I_{M}	2.13	act.	61	12	0.0	0.0085	0.1
I_{A}	2.14	act.	33	12	0.3	0.04	0.5
$I_{\mathrm{HVA}} + I_{\mathrm{K[Ca]}}$	2.15	act.	150	12	0	0.05	0.6
I_h	2.17	inact.	8.5	−48	0.8	–	–
I_{NaS}	2.18	act	200	−120	−0.08	0.0041	−0.48

Table 6.2 *Parameter values for ion channels presented in Chapter 2 for model linearized around* $-65\,\mathrm{mV}$ *for* $Rg_{\mathrm{k}} = 1$. *The action potential is assumed to consist of a pulse of* 1 ms *duration at* 0 mV. *The approximation to obtain* δ_x *and* b *is valid only when* $\tau_x(0\,\mathrm{mV})$ *is significantly larger than one millisecond.*

then several adaptation variables are needed, which leads to the model equations (6.1) and (6.2).

6.3.2 Spike-triggered adaptation arising from a biophysical ion channel

We have seen in Chapter 2 that some ion channels are partially open at the resting potential, while others react only when the membrane potential is well above the firing threshold. We now focus on the second group in order to give a biophysical interpretation of the jump amplitude b of a spike-triggered adaptation current.

Let us return to the example of a single ion channel of the Hodgkin and Huxley type such as the potassium current in Eq. (6.16). In contrast to the treatment earlier, we now study the change in the state of the ion channel induced during the large-amplitude excursion of the voltage trajectory during a spike. During the spike, the target $n_0(u)$ of the gating variable is close to 1; but since the time constant τ_n is long, the target is not reached during the short time that the voltage stays above the activation threshold. Nevertheless, the ion channel is partially activated by the spike. Unless the neuron is firing at a very large firing rate, each additional spike activates the channel further, always by the same amount Δ_n, which depends on the duration of the spike and the activation threshold of the current (Table 6.2). The spike-triggered jump in the adapting current w is then

$$b = \beta \Delta_n \,, \tag{6.21}$$

where $\beta = g_K\, p\, n_0(E_0)^{p-1}\,(E_0 - E_K)$ has been defined before.

Again, real neurons with their large quantity of ion channels have many adaptation currents w_k, each with its own time constant τ_k, subthreshold coupling a_k and spike-triggered jump b_k. The effective parameter values depend on the properties of the ion channels (Table 6.2).

https://doi.org/10.1017/CBO9781107447615.008 Published online by Cambridge University Press

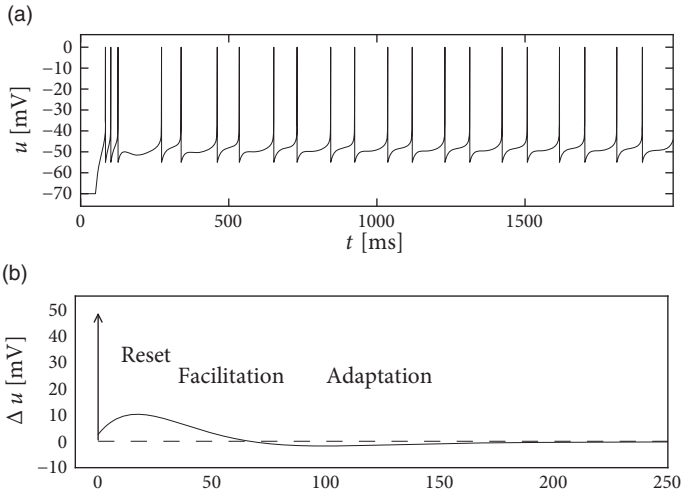

Fig. 6.10 Another type of bursting in a model with two spike-triggered currents. (a) Voltage trace of the neuron model Eqs. (6.3)–(6.4) with $u_{\rm reset} = -55\,{\rm mV}$, $\vartheta_{\rm rh} = -50\,{\rm mV}$, $b_1 = -12\,{\rm pA}$, $b_2 = 60\,{\rm pA}$, $\tau_1 = 20\,{\rm ms}$, $\tau_2 = 61\,{\rm ms}$, $a_1 = -3\,{\rm nS}$ and $a_2 = 0$. Parameters were chosen to correspond to a neuron coupled with a dendritic compartment and $I_{\rm M}$. (b) Voltage deflection brought by an isolated spike. Each spike brings first refractoriness, then a facilitation and finally adaptation on a longer time scale.

Example: Calculating the jump b of the spike-triggered adaptation current

We consider a gating dynamics

$$\frac{{\rm d}n}{{\rm d}t} = -\frac{n - n_0(u)}{\tau_n(u)}\,, \tag{6.22}$$

with the steplike activation function $n_0(u) = \Theta(u - u_0^{\rm act})$ where $u_0^{\rm act} = -30$ mV and $\tau_n(u) = 100$ ms independent of u. Thus, the gating variable n approaches a target value of 1 whenever the voltage u is above the activation threshold $u_0^{\rm act}$. Since the activation threshold of -30 mV is *above* the firing threshold (typically in the range of $-40\,{\rm mV}$) we can safely state that the neuron activation of the channel can only occur during an action potential. Assuming that during an action potential the voltage remains above $u_0^{\rm act}$ for $t = 1$ ms, we can integrate Eq. (6.22) and find that each spike causes an increase $\Delta_n = t/\tau_n$ where we have exploited that $t \ll \tau_n$. If we plug in the above numbers, we see that each spike causes an increase of n by a value of 0.01. If the duration of the spike were twice as long, the increase would be 0.02. After the spike the gating variable decays with the time constant τ_n back to zero. The increase Δ_n leads to a jump amplitude of the adaptation current given by Eq. (6.21).

https://doi.org/10.1017/CBO9781107447615.008 Published online by Cambridge University Press

6.3.3 Subthreshold adaptation caused by passive dendrites

While in the previous section, we have focused on the role of ion channels, here we show that a passive dendrite can also give rise to a subthreshold coupling of the form of Eq. (6.15).

We focus on a simple neuron model with two compartments, representing the soma and the dendrite, superscripts s and d respectively. The two compartments are both passive with membrane potential V^{s}, V^{d}, transversal resistance $R^{\mathrm{s}}_{\mathrm{T}}$, $R^{\mathrm{d}}_{\mathrm{T}}$, capacity C^{s}, C^{d} and resting potential u_{r}, E^{d}. The two compartments are linked by a longitudinal resistance R_{L} (see Chapter 3). If current is injected only in the soma, then the two-compartment model with passive dendrites corresponds to

$$\frac{\mathrm{d}}{\mathrm{d}t}V^{\mathrm{s}} = \frac{1}{C^{\mathrm{s}}}\left[-\frac{(V^{\mathrm{s}}-u_{\mathrm{rest}})}{R^{\mathrm{s}}_{\mathrm{T}}} - \frac{V^{\mathrm{s}}-V^{\mathrm{d}}}{R_{\mathrm{L}}} + I(t)\right], \tag{6.23}$$

$$\frac{\mathrm{d}}{\mathrm{d}t}V^{\mathrm{d}} = \frac{1}{C^{\mathrm{d}}}\left[-\frac{(V^{\mathrm{d}}-E^{\mathrm{d}})}{R^{\mathrm{d}}_{\mathrm{T}}} - \frac{V^{\mathrm{d}}-V^{\mathrm{s}}}{R_{\mathrm{L}}}\right]. \tag{6.24}$$

Such a system of differential equations can be mapped to the form of Eq. (6.15) by considering that the variable w represents the current flowing from the dendrite into the soma. In order to keep the treatment transparent, we assume that $E^{\mathrm{d}} = u_{\mathrm{rest}} = E$. In this case the adaptation current is $w = -(V^{\mathrm{d}} - u_{\mathrm{rest}})/R_{\mathrm{L}}$ and the two equations above reduce to

$$\tau^{\mathrm{eff}}\frac{\mathrm{d}V^{s}}{\mathrm{d}t} = -(V^{\mathrm{s}}-E) - R^{\mathrm{eff}}w \tag{6.25}$$

$$\tau_w\frac{\mathrm{d}w}{\mathrm{d}t} = a(V^{\mathrm{s}}-E) - w \tag{6.26}$$

with an effective input resistance $R^{\mathrm{eff}} = R^{\mathrm{s}}_{\mathrm{T}}/[1+(R^{\mathrm{s}}_{\mathrm{T}}/R_{\mathrm{L}})]$, an effective somatic time constant $\tau^{\mathrm{eff}} = C^{\mathrm{s}}R^{\mathrm{eff}}$, an effective adaptation time constant $\tau_w = R_{\mathrm{L}}C^{\mathrm{d}}/[1+(R_{\mathrm{L}}/R_{\mathrm{D}})]$ and a coupling between somatic voltage and adaptation current $a = -[R_{\mathrm{L}} + (R^2_{\mathrm{L}}/R_{\mathrm{D}})]^{-1}$.

There are three conclusions we should draw from this mapping. First, a is always negative, which means that passive dendrites introduce a *facilitating* subthreshold coupling. Second, facilitation is particularly strong with a small longitudinal resistance. Third, the timescale of the facilitation τ_w is smaller than the dendritic time constant $R^{\mathrm{d}}_{\mathrm{T}}C^{\mathrm{d}}$ – so that, compared with other "adaptation" currents, the dendritic current is a relatively fast one.

In addition to the subthreshold coupling discussed here, dendritic coupling can also lead to a spike-triggered current as we shall see in the next example.

Example: Bursting with a passive dendrite and I_{M}

Suppose that the action potential can be approximated by a 1 ms pulse at 0 mV. Then each spike brings an increase in the dendritic membrane potential. In terms of the

https://doi.org/10.1017/CBO9781107447615.008 Published online by Cambridge University Press

current w, the increase is $b = -aE_0(1 - e^{1\ \mathrm{ms}/\tau_w})$. Again, the spike-triggered jump is always negative, leading to spike-triggered facilitation. Figure 6.10 shows an example where we combined a dendritic compartment with the linearized effects of the M-current (Table 6.2) to result in regular bursting. The bursting is mediated by the dendritic facilitation which is counterbalanced by the adapting effects of I_M. The firing pattern looks different to the bursting in the AdEx (Fig. 6.4) as there is no alternation between detour and direct resets. Indeed, many different types of bursting are possible (see Izhikevich 2007a). This example (especially Fig. 6.10b) suggests that the dynamics of spike-triggered currents on multiple time scales can be understood in terms of their stereotypical effect on the membrane potential – and this insight is the starting point for the Spike Response Model in the next section.

6.4 Spike Response Model (SRM)

So far, we have described neuronal dynamics in terms of systems of differential equations. There is another approach that was introduced in Section 1.3.5 as the "filter picture." In this picture, the parameters of the model are replaced by (parametric) functions of time, generically called "filters." The neuron model is therefore interpreted in terms of a membrane filter as well as a function describing the shape of the spike (Fig. 6.11) and, potentially, also a function for the time course of the threshold. Together, these three functions establish the Spike Response Model (SRM).

The Spike Response Model is – just like the nonlinear integrate-and-fire models in Chapter 5 or the AdEx in Section 6.1 – a generalization of the leaky integrate-and-fire model. In contrast to nonlinear integrate-and-fire models, the SRM has no "intrinsic" firing threshold but only the sharp numerical threshold for reset. If the nonlinear function of the AdEx is fitted to experimental data, the transition between the linear subthreshold and superthreshold behavior is found to be rather abrupt, so that the nonlinear transition is, for most neurons, well approximated by a sharp threshold (see Fig. 5.3). Therefore, in the SRM, we work with a sharp threshold combined with a linear voltage equation.

While the SRM is therefore somewhat simpler than other models on the level of the spike generation mechanism, the subthreshold behavior of the SRM is richer than that of the integrate-and-fire model discussed so far and can account for various aspects of refractoriness and adaptation. In fact, the SRM combines the most general linear model with a sharp threshold.

It turns out that the integral formulation of the SRM is very useful for data fitting and also the starting point for the Generalized Linear Models in Chapter 9 and 10. Despite the apparent differences between integrate-and-fire models and the SRM, the leaky integrate-and-fire model, with or without adaptation variables, is a special case of the SRM. The relation of the SRM to integrate-and-fire models is the topic of Sections 6.4.3–6.4.4. We now start with a detailed explanation.

https://doi.org/10.1017/CBO9781107447615.008 Published online by Cambridge University Press

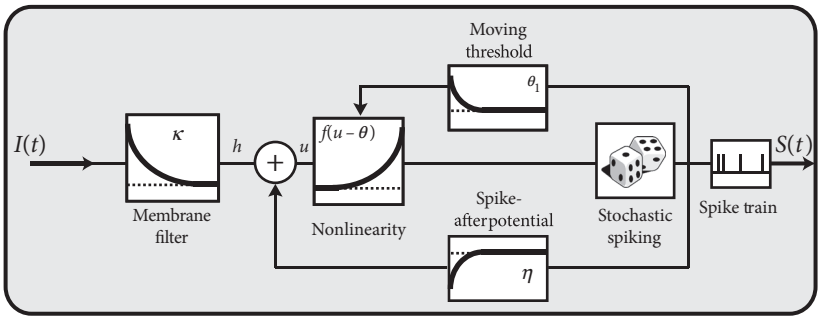

Fig. 6.11 Spike Response Model (SRM). Input current $I(t)$ is filtered with a filter $\kappa(s)$ and yields the input potential $h(t) = \int_0^\infty \kappa(s) I(t-s) \mathrm{d}s$. Firing occurs if the membrane potential u reaches the threshold ϑ. Spikes $S(t) = \sum_f \delta(t - t^f)$ are fed back into the threshold process in two distinct ways. Each spike causes an increase θ_1 of the threshold: $\vartheta(t) = \vartheta_0 + \int_0^\infty \theta_1(s) S(t-s) \mathrm{d}s$. Moreover, each spike generates a voltage contribution η to the membrane potential: $u(t) = h(t) + \int_0^\infty \eta(s) S(t-s) \mathrm{d}s$, where η captures the time course of the action potential and the spike-afterpotential; schematic figure.

6.4.1 Definition of the SRM

In the framework of the Spike Response Model (SRM) the state of a neuron is described by a single variable u which we interpret as the membrane potential. In the absence of input, the variable u is at its resting value, $u_{\rm rest}$. A short current pulse will perturb u and it takes some time before u returns to rest (Fig. 6.11). The function $\kappa(s)$ describes the time course of the voltage response to a short current pulse at time $s = 0$. Because the subthreshold behavior of the membrane potential is taken as linear, the voltage response h to an arbitrary time-dependent stimulating current $I^{\rm ext}(t)$ is given by the integral $h(t) = \int_0^\infty \kappa(s) I^{\rm ext}(t-s) \, \mathrm{d}s$.

Spike firing is defined by a threshold process. If the membrane potential reaches the threshold ϑ, an output spike is triggered. The form of the action potential and the afterpotential is described by a function η. Let us suppose that the neuron has fired some earlier spikes at times $t^f < t$. The evolution of u is given by

$$u(t) = \sum_f \eta(t - t^f) + \int_0^\infty \kappa(s) I^{\rm ext}(t-s) \, \mathrm{d}s + u_{\rm rest}. \tag{6.27}$$

The sum runs over all past firing times t^f with $f = 1, 2, 3, \ldots$ of the neuron under consideration. Introducing the spike train $S(t) = \sum_f \delta(t - t^f)$, Eq. (6.27) can be also written as a convolution

$$u(t) = \int_0^\infty \eta(s) S(t-s) \mathrm{d}s + \int_0^\infty \kappa(s) I^{\rm ext}(t-s) \, \mathrm{d}s + u_{\rm rest}. \tag{6.28}$$

In contrast to the leaky integrate-and-fire neuron discussed in Chapter 1 the threshold ϑ is not fixed, but time-dependent

$$\vartheta \quad \longrightarrow \quad \vartheta(t) \, . \tag{6.29}$$

https://doi.org/10.1017/CBO9781107447615.008 Published online by Cambridge University Press

Firing occurs whenever the membrane potential u reaches the dynamic threshold $\vartheta(t)$ from below

$$t = t^f \quad \Leftrightarrow \quad u(t) = \vartheta(t) \text{ and } \frac{\mathrm{d}[u(t) - \vartheta(t)]}{\mathrm{d}t} > 0\,. \tag{6.30}$$

Dynamic thresholds can be directly measured in experiments (Fuortes and Mantegazzini, 1962; Badel *et al.*, 2008a; Mensi *et al.*, 2012) and are a standard feature of phenomenological neuron models.

Example: Dynamic threshold – and how to get rid of it

A standard model of the dynamic threshold is

$$\vartheta(t) = \vartheta_0 + \sum_f \theta_1(t - t^f) = \vartheta_0 + \int_0^\infty \theta_1(s) S(t-s) \mathrm{d}s\,, \tag{6.31}$$

where ϑ_0 is the "normal" threshold of neuron i in the absence of spiking. After each output spike, the firing threshold of the neuron is increased by an amount $\theta_1(t - t^f)$ where $t^f < t$ denote the firing times in the past. For example, during an absolute refractory period Δ^{abs}, we may set θ_1 for a few milliseconds to a large and positive value so as to avoid any firing and let it relax back to zero over the next few hundred milliseconds; see Fig. 6.12a.

From a formal point of view, there is no need to interpret the variable u as the membrane potential. It is, for example, often convenient to transform the variable u so as to remove the time dependence of the threshold. In fact, a general Spike Response Model with arbitrary time-dependent threshold as in Eq. (6.31) can always be transformed into a Spike Response Model with fixed threshold ϑ_0 by a change of variables

$$\eta(t - t^f) \longrightarrow \eta^{\text{eff}}(t - t^f) = \eta(t - t^f) - \theta_1(t - t^f). \tag{6.32}$$

In other words, the dynamic threshold can be absorbed in the definition of the η kernel. Note, however, that in this case η can no longer be interpreted as the experimentally measured spike afterpotential, but must be interpreted as an "effective" spike afterpotential.

The argument can also be turned the other way round, so as to remove the spike afterpotential and only work with a dynamic threshold; see Fig. 6.12b. However, when an SRM is fitted to experimental data, it is convenient to separate the spike after-effects that are visible in the voltage trace (e.g., in the form of a hyperpolarizing spike-afterpotential, described by the kernel η), from the spike after-effects caused by an increase in the threshold which can be observed only *indirectly* via the absence of spike firing. Whereas the prediction of spike times is insensitive to the relative contribution of η and θ_1, the prediction of the subthreshold voltage time course is not. Therefore, it is useful to explicitly work with two distinct adapatation mechanisms in the SRM (Mensi *et al.*, 2012).

https://doi.org/10.1017/CBO9781107447615.008 Published online by Cambridge University Press

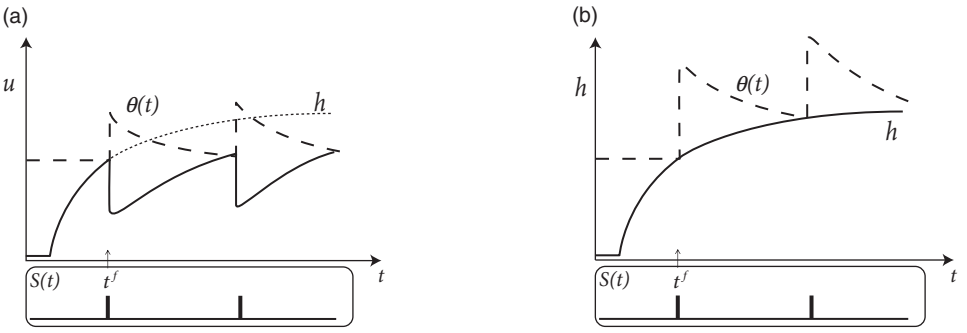

Fig. 6.12 Spike-afterpotential and dynamic threshold in the SRM. (a) At time t^f a spike occurs because the membrane potential hits the threshold $\vartheta(t)$. The threshold jumps to a higher value (dashed line) and, at the same time, a contribution $\eta(t-t^f)$ is added to the membrane potential, i.e., the spike and its spike-afterpotential are "pasted" into the picture. If no further spikes are triggered, the threshold decays back to its resting value and the spike-afterpotential decays back to zero. The total membrane potential (thick solid line) after a spike is $u(t) = h(t) + \sum_f \eta(t-t^f)$ where $h(t)$ is the input potential (thin dotted line). (b) If the model is used to predict spike times, but not the membrane potential, the spike-afterpotential η can be integrated into the dynamic threshold so that $u(t) = h(t)$. At the moment of spiking the value of the threshold is increased, but the membrane potential is not affected (either through reset or spike-afterpotential).

6.4.2 *Interpretation of* η *and* κ

So far Eq. (6.27) in combination with the threshold condition (6.30) defines a mathematical model. Can we give a biological interpretation of the terms?

The kernel $\kappa(s)$ is the *linear response* of the membrane potential to an input current. It describes the time course of a deviation of the membrane potential from its resting value that is caused by a short current pulse ("impulse response").

The kernel η describes the standard form of an action potential of neuron i including the negative overshoot which typically follows a spike (the spike-afterpotential). Graphically speaking, a contribution η is "pasted in" each time the membrane potential reaches the threshold ϑ (Fig. 6.12a). Since the form of the spike is always the same, the exact time course of the action potential carries no information. What matters is whether there is the event "spike" or not. The event is fully characterized by the firing time t^f.

In a simplified model, the *form* of the action potential may therefore be neglected as long as we keep track of the firing times t^f. The kernel η then describes simply the "reset" of the membrane potential to a lower value after the spike at t^f just as in the integrate-and-fire model

$$\eta(t-t^f) = -\eta_0 \exp\left(-\frac{t-t^f}{\tau_{\rm recov}}\right), \tag{6.33}$$

https://doi.org/10.1017/CBO9781107447615.008 Published online by Cambridge University Press

with a parameter $\eta_0 > 0$. The spike-afterpotential decays back to zero with a recovery time constant $\tau_{\rm recov}$. The leaky integrate-and-fire model is in fact a special case of the SRM, with parameter $\eta_0 = (\vartheta - u_r)$ and $\tau_{\rm recov} = \tau_m$.

Example: Refractoriness

Refractoriness may be characterized experimentally by the observation that immediately after a first action potential it is impossible (absolute refractoriness) or more difficult (relative refractoriness) to excite a second spike. In Fig. 5.5. we have already seen that refractoriness shows up as increased firing threshold and increased conductance immediately after a spike.

Absolute refractoriness can be incorporated in the SRM by setting the dynamic threshold during a time $\Delta^{\rm abs}$ to an extremely high value that cannot be attained.

Relative refractoriness can be mimicked in various ways. First, after a spike the firing threshold returns only slowly back to its normal value (increase in firing threshold). Second, after the spike the membrane potential, and hence η, passes through a regime of hyperpolarization (spike-afterpotential) where the voltage is *below* the resting potential. During this phase, more stimulation than usual is needed to drive the membrane potential above threshold. In fact, this is equivalent to a transient increase of the firing threshold (see above).

Third, the responsiveness of the neuron is reduced immediately after a spike. In the SRM we can model the reduced responsiveness by making the shape of ε and κ depend on the time since the *last* spike timing $\hat{t}$.

We label output spikes such that the most recent one receives the label t^1 (i.e., $t > t^1 > t^2 > t^3 \ldots$). This means that, after each firing event, output spikes need to be relabeled. The advantage, however, is that the *last* output spike always keeps the label t^1. For simplicity, we often write $\hat{t}$ instead of t^1 to denote the most recent spike.

With this notation, a slightly more general version of the Spike Response Model is

$$u(t) = \sum_f \eta(t - t^f) + \int_0^\infty \kappa(t - \hat{t}, s)\, I^{\rm ext}(t - s)\, {\rm d}s + u_{\rm rest}\,. \tag{6.34}$$

6.4.3 Mapping the integrate-and-fire model to the SRM

In this section, we show that the leaky integrate-and-fire neuron with adaptation defined above in Eqs. (6.7) and (6.8) is a special case of the Spike Response Model. Let us recall that the leaky integrate-and-fire model follows the equation of a linear circuit with resistance R and capacity C

$$\tau_m \frac{{\rm d}u_i}{{\rm d}t} = -(u_i - E_0) - R \sum_k w_k + R I_i(t), \tag{6.35}$$

https://doi.org/10.1017/CBO9781107447615.008 Published online by Cambridge University Press

where $\tau_m = RC$ is the time constant, E_0 the leak reversal potential, w_k are adaptation variables, and I_i is the input current to neuron i. At each firing time

$$\{t_i^f\} \in \{t | u_i(t) = \vartheta\}\,, \tag{6.36}$$

the voltage is reset to a value u_r. At the same time, the adaptation variables are increased by an amount b_k

$$\tau_k \frac{\mathrm{d}w_k}{\mathrm{d}t} = a_k\,(u_i - E_0) - w_k + \tau_k\, b_k \sum_{t^f} \delta(t - t^f). \tag{6.37}$$

The equations of the adaptive leaky integrate-and-fire model, Eqs. (6.35) and (6.37), can be classified as *linear* differential equations. However, because of the reset of the membrane potential after firing, the integration is not completely trivial. In fact, there are two different ways of proceeding with the integration. The first method is to treat the reset after each firing as a new initial condition – this is the procedure typically chosen for a numerical integration of the model. Here we follow a different path and describe the reset as a current pulse. As we shall see, the result enables a mapping of the leaky integrate-and-fire model to the SRM.

Let us consider a short current pulse $I_i^{\text{out}} = -q\,\delta(t)$ applied to the RC circuit. It removes a charge q from the capacitor C and lowers the potential by an amount $\Delta u = -q/C$. Thus, a reset of the membrane potential from a value of $u = \vartheta$ to a new value $u = u_r$ corresponds to an "output" current pulse which removes a charge $q = C\,(\vartheta - u_r)$. The reset takes place every time when the neuron fires. The total reset current is therefore

$$I_i^{\text{out}}(t) = -C\,(\vartheta - u_r) \sum_f \delta(t - t_i^f)\,, \tag{6.38}$$

where the sum runs over all firing times t_i^f. We add the output current (6.38) on the right-hand side of (6.35),

$$\tau_m \frac{\mathrm{d}u_i}{\mathrm{d}t} = -(u_i - E_0) - R \sum_k w_k + R I_i(t) - RC\,(\vartheta - u_r) \sum_f \delta(t - t_i^f)\,, \tag{6.39}$$

$$\tau_k \frac{\mathrm{d}w_k}{\mathrm{d}t} = a_k\,(u_i - E_0) - w_k + \tau_k\, b_k \sum_{t^f} \delta(t - t^f). \tag{6.40}$$

Since Eqs. (6.39) and (6.40) define a system of linear equations, we can integrate each term separately and superimpose the result at the end. To perform the integration, we proceed in three steps. First, we shift the voltage so as to set the equilibrium potential to zero. Second, we calculate the eigenvalues and eigenvectors of the "free" equations in the absence of input (and therefore no spikes). If there are K adaptation variables, we have a total of $K+1$ eigenvalues which we label as $\lambda_1, \lambda_2, \ldots$ The associated eigenvectors are e_k with components $(e_{k0}, e_{k1}, \ldots, e_{kK})^T$. Third, we express the response to an impulse $\Delta u = 1$ in the voltage (no perturbation in the adaptation variables) in terms of the $K+1$ eigenvectors: $(1,0,0,\ldots,0)^T = \sum_{k=0}^{K} \beta_k e_k$. Finally, we express the pulse caused by a reset of

https://doi.org/10.1017/CBO9781107447615.008 Published online by Cambridge University Press

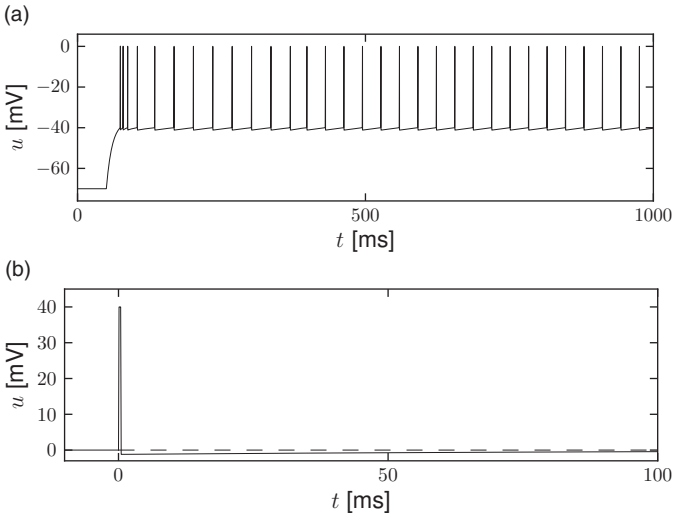

Fig. 6.13 SRM with a choice of η leading to adaptation. (a) The response of the neuron model to injection of a step current. (b) The spike-afterpotential η with adaptation time constant $\tau_w = 100$ ms. A short (0.5 ms) period at +40 mV replaces the stereotypical shape of the action potential.

voltage and adaptation variables in terms of the eigenvectors $(-\vartheta + u_r, b_1, b_2, \ldots, b_K)^T = \sum_{k=0}^{K} \gamma_k e_k$.

The response to the reset pulses yields the kernel η while the response to voltage pulses yields the filter $\kappa(s)$ of the SRM

$$u_i(t) = \sum_f \eta(t - t_i^f) + \int_0^\infty \kappa(s)\, I_i(t-s)\, \mathrm{d}s\,, \tag{6.41}$$

with kernels

$$\eta(s) = \sum_{k=0}^{K} \gamma_k e_{k0} \exp(\lambda_k s) \Theta(s)\,, \tag{6.42}$$

$$\kappa(s) = \sum_{k=0}^{K} \beta_k e_{k0} \exp(\lambda_k s)\, \Theta(s). \tag{6.43}$$

As usual, $\Theta(x)$ denotes the Heaviside step function.

Example: Adaptation and bursting

Let us first study a leaky integrate-and-fire model with a single slow adaptation variable $\tau_w \gg \tau_m$ which is coupled to the voltage in the subthreshold regime ($a > 0$) and

https://doi.org/10.1017/CBO9781107447615.008 Published online by Cambridge University Press

increased during spiking by an amount b. In this case there are only two equations, one for the voltage and one for adaptation, so that the eigenvectors and eigenvalues can be calculated "by hand." With a parameter $\delta = \tau_m/\tau_w \ll 1$, the eigenvalues are $\lambda_1 = -\tau_w[1 - a\,\delta]$ and $\lambda_2 = -\tau_w\,\delta\,[1 + a]$, associated to eigenvectors $e_1 = (1, a\,\delta)^{\mathrm{T}}$ and $e_2 = (1, -1 + \delta + a\,\delta)^{\mathrm{T}}$. The resulting spike-afterpotential kernel $\eta(s)$ is shown in Fig. 6.13b. Because of the slow time constant $\tau_w \gg \tau_m$, the kernel η has a long hyperpolarizing tail. The neuron model responds to a step current with adaptation, because of accumulation of hyperpolarizing spike-afterpotentials over many spikes.

As a second example, we consider four adaptation currents with different time constants $\tau_1 < \tau_2 < \tau_3 < \tau_4$. We assume pure spike-triggered coupling ($a = 0$) so that the integration of the differential equations of w_k gives each an exponential current

$$w_k(t) = \sum_f b_k \exp\left(-\frac{t - t^f}{\tau_k}\right) \Theta(t - t^f). \tag{6.44}$$

We choose the time constant of the first current to be very short and $b_1 < 0$ (inward current) so as to model the upswing of the action potential (a candidate current would be sodium). A second current (e.g., a fast potassium channel) with a slightly longer time constant is outgoing ($b_2 > 0$) and leads to the downswing and rapid reset of the membrane potential. The third current, with a time constant of tens of milliseconds, is inward ($b_3 < 0$), while the slowest current is again hyperpolarizing ($b_4 > 0$). Integration of the voltage equation with all four currents generates the spike-afterpotential η shown Fig. 6.14b. Because of the depolarizing spike-afterpotential induced by the inward current w_3, the neuron model responds to a step current of appropriate amplitude with bursts. The bursts end because of the accumulation of the hyperpolarizing effect of the slowest current.

6.4.4 Multi-compartment integrate-and-fire model as an SRM (*)

The models discussed in this chapter are point neurons, i.e., models that do not take into account the spatial structure of a real neuron. In Chapter 3 we have already seen that the electrical properties of dendritic trees can be described by compartmental models. In this section, we want to show that neurons with a linear dendritic tree and a voltage threshold for spike firing at the soma can be mapped to the Spike Response Model.

We study an integrate-and-fire model with a passive dendritic tree described by n compartments. Membrane resistance, core resistance, and capacity of compartment μ are denoted by R_{T}^{μ}, R_{L}^{μ}, and C^{μ}, respectively. The longitudinal core resistance between compartment μ and a neighboring compartment ν is $r^{\mu\nu} = (R_{\mathrm{L}}^{\mu} + R_{\mathrm{L}}^{\nu})/2$; see Fig. 3.8. Compartment $\mu = 1$ represents the soma and is equipped with a simple mechanism for spike generation, i.e., with a threshold criterion as in the standard integrate-and-fire model. The remaining dendritic compartments ($2 \le \mu \le n$) are passive.

https://doi.org/10.1017/CBO9781107447615.008 Published online by Cambridge University Press

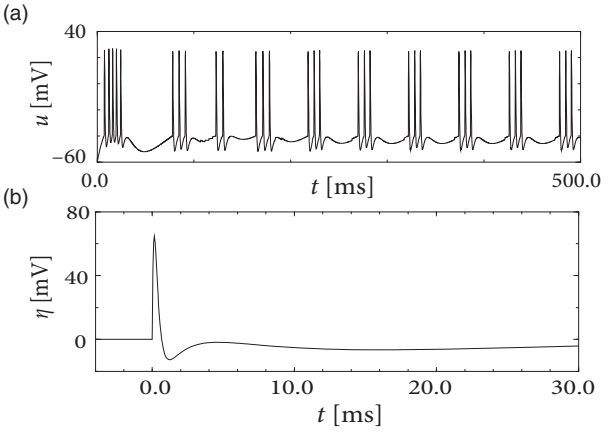

Fig. 6.14 SRM with choice of η leading to bursting. (a) The refractory kernel η of an integrate-and-fire model with four spike-triggered currents. (b) The voltage response to a step current exhibits bursting. Adapted from Gerstner *et al*. (1996b).

Each compartment $1 \leq \mu \leq n$ of neuron i may receive input $I_i^\mu(t)$ from presynaptic neurons. As a result of spike generation, there is an additional reset current $\Omega_i(t)$ at the soma. The membrane potential V_i^μ of compartment μ is given by

$$\frac{\mathrm{d}}{\mathrm{d}t} V_i^\mu = \frac{1}{C_i^\mu} \left[-\frac{V_i^\mu}{R_{\mathrm{T},i}^\mu} - \sum_\nu \frac{V_i^\mu - V_i^\nu}{r_i^{\mu\nu}} + I_i^\mu(t) - \delta^{\mu 1}\, \Omega_i(t) \right], \tag{6.45}$$

where the sum runs over all neighbors of compartment μ. The Kronecker symbol $\delta^{\mu\nu}$ equals unity if the upper indices are equal; otherwise, it is zero. The subscript i is the index of the neuron; the upper indices μ or ν refer to compartments. Below we will identify the somatic voltage V_i^1 with the potential u_i of the Spike Response Model.

Equation (6.45) is a system of linear differential equations if the external input current is independent of the membrane potential. The solution of Eq. (6.45) can thus be formulated by means of Green's functions $G_i^{\mu\nu}(s)$ that describe the impact of a current pulse injected in compartment ν on the membrane potential of compartment μ. The solution is of the form

$$V_i^\mu(t) = \sum_\nu \frac{1}{C_i^\nu} \int_0^\infty G_i^{\mu\nu}(s) \left[I_i^\nu(t-s) - \delta^{\nu 1}\, \Omega_i(t-s) \right] \mathrm{d}s\,. \tag{6.46}$$

Explicit expressions for the Green's function $G_i^{\mu\nu}(s)$ for arbitrary geometry have been derived by Abbott *et al*. (1991) and Bressloff and Taylor (1994).

We consider a network made up of a set of neurons described by Eq. (6.45) and a simple threshold criterion for generating spikes. We assume that each spike t_j^f of a presynaptic neuron j evokes, for $t > t_j^f$, a synaptic current pulse $\alpha(t - t_j^f)$ into the postsynaptic neuron i. The actual amplitude of the current pulse depends on the strength W_{ij} of the synapse that

https://doi.org/10.1017/CBO9781107447615.008 Published online by Cambridge University Press

connects neuron j to neuron i. The total input to compartment μ of neuron i is thus

$$I_i^\mu(t) = \sum_{j \in \Gamma_i^\mu} W_{ij} \sum_f \alpha(t - t_j^f). \tag{6.47}$$

Here, Γ_i^μ denotes the set of all neurons that have a synapse with compartment μ of neuron i. The firing times of neuron j are denoted by t_j^f.

In the following we assume that spikes are generated at the soma in the manner of the integrate-and-fire model. That is to say, a spike is triggered as soon as the somatic membrane potential reaches the firing threshold, ϑ. After each spike the somatic membrane potential is reset to $V_i^1 = u_r < \vartheta$. This is equivalent to a current pulse

$$\gamma_i(s) = C_i^1 (\vartheta - u_r) \delta(s), \tag{6.48}$$

so that the overall current due to the firing of action potentials at the soma of neuron i amounts to

$$\Omega_i(t) = \sum_f \gamma_i(t - t_i^f). \tag{6.49}$$

We will refer to Eqs. (6.46)–(6.49) together with the threshold criterion for generating spikes as the multi-compartment integrate-and-fire model.

Using the above specializations for the synaptic input current and the somatic reset current the membrane potential (6.46) of compartment μ in neuron i can be rewritten as

$$V_i^\mu(t) = \sum_f \eta_i^\mu(t - t_i^f) + \sum_\nu \sum_{j \in \Gamma_i^\nu} W_{ij} \sum_f \varepsilon_i^{\mu\nu}(t - t_j^f), \tag{6.50}$$

with

$$\varepsilon_i^{\mu\nu}(s) = \frac{1}{C_i^\nu} \int_0^\infty G_i^{\mu\nu}(s') \, \alpha(s - s') \, \mathrm{d}s', \tag{6.51}$$

$$\eta_i^\mu(s) = \frac{1}{C_i^1} \int_0^\infty G_i^{\mu 1}(s') \, \gamma_i(s - s') \, \mathrm{d}s'. \tag{6.52}$$

The kernel $\varepsilon_i^{\mu\nu}(s)$ describes the effect of a presynaptic action potential arriving at compartment ν on the membrane potential of compartment μ. Similarly, $\eta_i^\mu(s)$ describes the response of compartment μ to an action potential generated at the soma.

The triggering of action potentials depends on the *somatic* membrane potential only. We define $u_i = V_i^1$, $\eta_i(s) = \eta_i^1(s)$ and, for $j \in \Gamma_i^\nu$, we set $\varepsilon_{ij} = \varepsilon_i^{1\nu}$. This yields the equation of the SRM

$$u_i(t) = \sum_f \eta_i(t - t_i^f) + \sum_j W_{ij} \sum_f \varepsilon_{ij}(t - t_j^f). \tag{6.53}$$

Example: Two-compartment integrate-and-fire model

We illustrate the methodology by mapping a simple model with two compartments and a reset mechanism at the soma (Rospars and Lansky, 1993) to the Spike Response

https://doi.org/10.1017/CBO9781107447615.008 Published online by Cambridge University Press

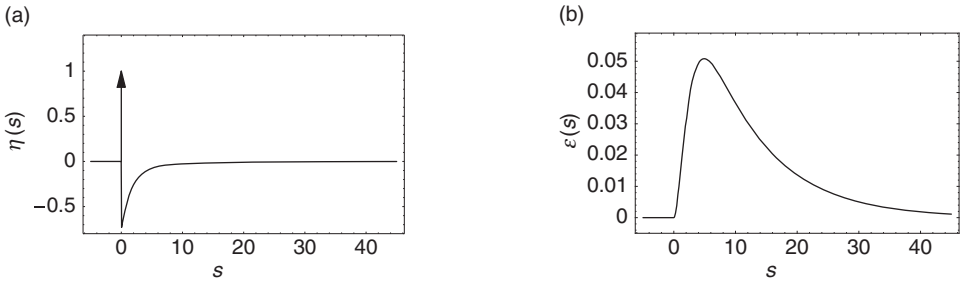

Fig. 6.15 Two-compartment integrate-and-fire model. (a) Response kernel $\eta_0(s)$ of a neuron with two compartments and a fire-and-reset threshold dynamics. The response kernel is a double exponential with time constants $\tau_{12} = 2$ ms and $\tau_0 = 10$ ms. The spike at $s = 0$ is indicated by a vertical arrow. (b) Response kernel $\varepsilon_0(s)$ for excitatory synaptic input at the dendritic compartment with a synaptic time constant $\tau_s = 1$ ms. The response kernel is a superposition of three exponentials and exhibits the typical time course of an excitatory postsynaptic potential.

Model. The two compartments are characterized by a somatic capacitance C^1 and a dendritic capacitance $C^2 = aC^1$. The membrane time constant is $\tau_0 = R^1 C^1 = R^2 C^2$ and the longitudinal time constant $\tau_{12} = r^{12} C^1 C^2/(C^1 + C^2)$. The neuron fires if $V^1(t) = \vartheta$. After each firing the somatic potential is reset to u_r. This is equivalent to a current pulse

$$\gamma(s) = q\,\delta(s)\,, \tag{6.54}$$

where $q = C^1\,[\vartheta - u_r]$ is the charge lost during the spike. The dendrite receives spike trains from other neurons j and we assume that each spike evokes a current pulse with time course

$$\alpha(s) = \frac{1}{\tau_s} \exp\left(-\frac{s}{\tau_s}\right) \Theta(s)\,. \tag{6.55}$$

For the two-compartment model it is straightforward to integrate the equations and derive the Green's function. With the Green's function we can calculate the response kernels $\eta_0(s) = \eta_i^{(1)}$ and $\varepsilon_0(s) = \varepsilon_i^{12}$ as defined in Eqs. (6.51) and (6.52). We find

$$\eta_0(s) = -\frac{\vartheta - u_r}{(1+a)} \exp\left(-\frac{s}{\tau_0}\right) \left[1 + a \exp\left(-\frac{s}{\tau_{12}}\right)\right], \tag{6.56}$$

$$\varepsilon_0(s) = \frac{1}{(1+a)} \exp\left(-\frac{s}{\tau_0}\right) \left[\frac{1 - \mathrm{e}^{-\delta_1 s}}{\tau_s\,\delta_1} - \exp\left(-\frac{s}{\tau_{12}}\right) \frac{1 - \mathrm{e}^{-\delta_2 s}}{\tau_s\,\delta_2}\right],$$

with $\delta_1 = \tau_s^{-1} - \tau_0^{-1}$ and $\delta_2 = \tau_s^{-1} - \tau_0^{-1} - \tau_{12}^{-1}$. Figure 6.15 shows the two response kernels with parameters $\tau_0 = 10$ ms, $\tau_{12} = 2$ ms, and $a = 10$. The synaptic time constant is $\tau_s = 1$ ms. The kernel $\varepsilon_0(s)$ describes the voltage response of the soma to an input at the dendrite. It shows the typical time course of an excitatory or inhibitory postsynaptic

https://doi.org/10.1017/CBO9781107447615.008 Published online by Cambridge University Press

potential. The time course of the kernel $\eta_0(s)$ is a double exponential and reflects the dynamics of the reset in a two-compartment model.

6.5 Summary

By adding one or several adaptation variables to integrate-and-fire models, a large variety of firing patterns found in real neurons, such as adaptation, bursting or initial bursting, can be explained. The dynamics of the adaptation variables has two components: (i) a coupling to the voltage u via a parameter a which provides subthreshold adaptation and, in nonlinear neuron models, also a contribution to spike-triggered adaptation; and (ii) an explicit spike-triggered adaptation via an increase of the adaptation current during each firing by an amount b. While positive values for a and b induce a hyperpolarization of the membrane and therefore lead to spike-frequency adaptation, negative values induce a depolarization and lead to delayed onset of spiking and spike frequency facilitation. Bursting is most easily achieved by a suitable combination of the reset parameters u_r and b.

The phenomenological adaptation variables w_k can be derived from the ionic currents flowing through different ion channels. Coupling of an integrate-and-fire model to a passive dendrite also yields effective adaptation variables which have, however, a facilitating influence.

The adaptation variables can be combined with a quadratic integrate-and-fire model which leads to the Izhikevich model; with an exponential integrate-and-fire model which leads to the AdEx model; or with a leaky integrate-and-fire model. In the latter case, the differential equations can be analytically integrated in the presence of an arbitrary number of adaptation variable. Integration leads to the Spike Response Model (SRM) which presents a general linear model combined with a sharp firing threshold. The Spike Response Model is the starting point for the Generalized Linear Models in the presence of noise which we will introduce in Chapter 9.

Literature

Formal neuron models where spikes are triggered by a threshold process were popular in the 1960s (Stein, 1965, 1967b; Geisler and Goldberg, 1966; Weiss, 1966), but the ideas can be traced back much earlier (Lapicque, 1907; Hill, 1936). It was recognized early that these models lend themselves for hardware implementations (French and Stein, 1970) and mathematical analysis (Stein, 1965, 1967a), and can be fitted to experimental data (Brillinger, 1988, 1992).

Dynamic thresholds that increase after each spike have been a standard feature of phenomenological neuron models for a long time (Fuortes and Mantegazzini, 1962; Geisler and Goldberg, 1966; Weiss, 1966) and so have the slow subthreshold processes of adaptation (Sabah and Leibovic, 1969; Mauro *et al.*, 1970; Fishman *et al.*, 1977; Sirovich

and Knight, 1977). While the linear subthreshold coupling of voltage and adaptation currents via a coupling parameter a is nicely presented and analyzed in Richardson *et al*. (2003), the spike-triggered jump b of the adaptation current has been mainly popularized by Izhikevich (2003) – but can be found in earlier papers (e.g., Gerstner *et al*., 1996b; Liu and Wang, 2001), and much earlier in the form of a spike-triggered increase in the threshold (Fuortes and Mantegazzini, 1962; Geisler and Goldberg, 1966; Weiss, 1966).

The phase plane analysis of the AdEx model presented in this chapter is based on Naud *et al*. (2008). The main difference between the AdEx model (Brette and Gerstner, 2005) and the highly influential model of Izhikevich (2003) is that the AdEx uses in the voltage equation an exponential nonlinearity (as suggested by experiments (Badel *et al*., 2008a)) whereas the Izhikevich model uses a quadratic nonlinearity (as suggested by bifurcation analysis close to the bifurcation point (Ermentrout, 1996)).

The book by Izhikevich (2007a) as well as the Scholarpedia articles on the Spike Response Model (SRM) and the adaptive exponential integrate-and-fire (AdEx) model (Gerstner, 2008; Gerstner and Brette, 2009), present readable reviews of the model class discussed in this chapter.

The functions η, κ, and ε_{ij} are *response kernels* that describe the effect of spike emission and spike reception on the variable u_i. This interpretation has motivated the name "Spike Response Model." While the name and the specific formulation of the model equations (6.27)–(6.30) has been used since 1995 (Gerstner, 1995; Gerstner *et al*., 1996b; Kistler *et al*., 1997), closely related models can be found in earlier works; see, e.g., Hill (1936); Geisler and Goldberg (1966).

Exercises

1. **Time scale of firing rate decay**. *The characteristic feature of adaptation is that, after the onset of a superthreshold step current, interspike intervals become successively longer, or, equivalently, the momentary firing rate drops. The aim is to make a quantitative prediction of the decay of the firing rate of a leaky integrate-and-fire model with a single adaptation current.*

   (a) Show that the firing rate of Eqs. (6.7) *and* (6.8) *with constant I, constant w and* $a = 0$ *is*

$$f(I,w) = -\left[\tau_m \log\left(1 - \frac{\vartheta_{\rm rh} - u_{\rm reset}}{R(I-w)}\right)\right]^{-1}. \tag{6.57}$$

   (b) For each spike (i.e., once per interspike interval), w jumps by an amount b. Show that for I constant and w averaged over one interspike interval, Eq. (6.8) *becomes:*

$$\tau_w \frac{{\rm d}w}{{\rm d}t} = -w + b\tau_w f(I,w). \tag{6.58}$$

   (c) At time t_0*, a strong current of amplitude* I_0 *is switched on that causes transiently a firing rate* $f \gg \tau_w$*. Afterward the firing rate decays. Find the effective time constant of the firing rate for the case of strong input current.*

   Hint: Start from Eq. (6.58) *and consider a Taylor expansion of* $f(I,w)$.

2. **Subthreshold resonance**. *We study a leaky integrate-and-fire model with a single adaptation variable w.*

   (a) Assume $E_0 = u_{\rm rest}$ *and cast equation Eqs.* (6.7) *and* (6.8) *in the form of Eq.* (6.27). *Set*

https://doi.org/10.1017/CBO9781107447615.008 Published online by Cambridge University Press

$\varepsilon = 0$ *and calculate* η *and* κ. *Show that* $\kappa(t)$ *can be written as a linear combination* $\kappa(t) = k_+ e^{\lambda_+ t} + k_- e^{\lambda_- t}$ *with*

$$\lambda_\pm = \frac{1}{2\tau_m \tau_w}\left(-(\tau_m + \tau_w) \pm \sqrt{\tau_m + \tau_w - 4\tau_m \tau_w (1 + aR)}\right) \tag{6.59}$$

and

$$k_\pm = \pm \frac{R(\lambda_\pm \tau_w + 1)}{\tau_m \tau_w (\lambda_+ - \lambda_-)}. \tag{6.60}$$

(b) What are the parameters of Eqs. (6.7)–(6.8) *that lead to oscillations in* $\kappa(t)$*?*
(c) What is the frequency of the oscillation?
Hint: Section 4.4.3.
(d) Take the Fourier transform of Eqs. (6.7)–(6.8) *and find the function* $\hat{R}(\omega)$ *that relates the current* $\hat{I}(\omega)$ *at frequency* ω *to the voltage* $\hat{u}(\omega)$ *at the same frequency, i.e.,* $\hat{u}(\omega) = \hat{R}(\omega)\hat{I}(\omega)$. *Show that, in the case where* κ *has oscillations, the function* $\hat{R}(\omega)$ *has a global maximum. What is the frequency where this happens?*

3. **Integrate-and-fire model with slow adaptation.**
The aim is to relate the leaky integrate-and-fire model with a single adaptation variable, defined in Eqs. (6.7) *and* (6.8), *to the Spike Response Model in the form of Eq.* (6.27). *Adaptation is slow so that* $\tau_m/\tau_w = \delta \ll 1$ *and all calculations can be done to first order in* δ.
(a) Show that the spike-afterpotential is given by

$$\eta(t) = \gamma_1 e^{\lambda_1 t} + \gamma_2 e^{\lambda_2 t}, \tag{6.61}$$

$$\gamma_1 = \Delta u\,(1 - \delta - \delta a) - b\,(1 + \delta), \tag{6.62}$$

$$\gamma_2 = \Delta u - \gamma_1. \tag{6.63}$$

(b) Derive the input response kernel $\kappa(s)$.
Hint: Use the result from (a).

4. **Integrate-and-fire model with time-dependent time constant**. *Since many channels are open immediately after a spike, the effective membrane time constant after a spike is smaller than the time constant at rest. Consider an integrate-and-fire model with spike-time-dependent time constant, i.e., with a membrane time constant* τ *that is a function of the time since the last post-synaptic spike,*

$$\frac{du}{dt} = -\frac{u}{\tau(t - \hat{t})} + \frac{1}{C} I^{\text{ext}}(t); \tag{6.64}$$

see Wehmeier et al. (1989); Stevens and Zador (1998). As usual, $\hat{t}$ *denotes the last firing time of the neuron. The neuron fires if* $u(t)$ *hits a fixed threshold* ϑ *and integration restarts with a reset value* u_r.
(a) Suppose that the time constant is $\tau(t - \hat{t}) = 2\,\text{ms}$ *for* $t - \hat{t} < 10\,\text{ms}$ *and* $\tau(t - \hat{t}) = 20\,\text{ms}$ *for* $t - \hat{t} \geq 10\,\text{ms}$. *Set* $u_r = -10\,\text{mV}$. *Sketch the time course of the membrane potential for an input current* $I(t) = q\,\delta(t - t')$ *arriving at* $t' = 5\,\text{ms}$ *or* $t' = 15\,\text{ms}$. *What are the differences between the two cases?*
(b) Integrate Eq. (6.64) *for arbitrary input with* $u(\hat{t}) = u_r$ *as initial condition and interpret the result.*

5. **Spike-triggered adaptation currents**. *Consider a leaky integrate-and-fire model. A spike at time* t^f *generates several adaptation currents* $dw_k/dt = -\frac{w_k}{\tau_k} + b_k \delta(t - t^f)$ *with* $k = 1, \ldots, K$.
(a) Calculate the effect of the adaptation current on the voltage.
(b) Construct a combination of spike-triggered currents that could generate slow adaptation.
(c) Construct a combination of spike-triggered currents that could generate bursts.

https://doi.org/10.1017/CBO9781107447615.008 Published online by Cambridge University Press